



PackquID: In-packet Liquid Identification Using RF Signals

FEI SHANG, PANLONG YANG*, YUBO YAN, and XIANG-YANG LI, CAS Key Laboratory of Wireless-Optical Communications, School of Computer Science and Technology, University of Science and Technology of China, China

There are many scenarios where the liquid is occluded by other items (*e.g.* books in a packet), in which existing RF-based liquid identification methods are generally not suitable. Moreover, status methods are not applicable when the height of the liquid to be tested changes. This paper proposes *PackquID*, an RF-based in-packet liquid identification system, which can identify liquid without prior knowledge. In dealing with the obstruction of other items and the unknown container, we utilize a dual-antenna model and craft a relative frequency response factor, exploring the diversity of the permittivity in the frequency domain. In tackling the variable liquid height, we extend our model to 3D scope by analyzing the electric field distribution and solving the height effect via spatial-differential model. With 500 pages of printer paper obscured, *PackquID* can identify 9 common liquids, including Coca-Cola and Pepsi, with an accuracy of over 86% for 4 different packets (canvas bag, paper bag, backpack, and box) and 4 different containers. Nevertheless, *PackquID* can still identify liquids with an accuracy rate of over 87%, even when the liquid height changes from 4 cm to 12 cm.

CCS Concepts: • Human-centered computing → Ubiquitous and mobile computing design and evaluation methods.

Additional Key Words and Phrases: Wireless sensing; Liquid identification; Electromagnetic waves; Complex permittivity

ACM Reference Format:

Fei Shang, Panlong Yang, Yubo Yan, and Xiang-Yang Li. 2022. PackquID: In-packet Liquid Identification Using RF Signals. *Proc. ACM Interact. Mob. Wearable Ubiquitous Technol.* 6, 4, Article 181 (December 2022), 27 pages. <https://doi.org/10.1145/3569469>

181

1 INTRODUCTION

Liquid identification has a wide range of application scenarios, such as subway security inspections and large gatherings to detect whether participants are carrying flammable liquids. Traditional identification methods usually require expensive specialized equipments, such as spectrometers [6, 14, 16, 42, 46], which accurately inconvenient to deploy. As a result, these methods are not suitable for ubiquitous liquid testing, whose potential application scenarios range from monitoring daily nutrition intake from drinks, identification of fake luxury perfume, detection of water contamination in countries with limited sanitary water facilities, safety inspection in public transportation, in-home urine testing to track disease progression, etc [26].

For easy deployment, recently, a lot of meaningful work [15, 24, 25, 45, 58, 59, 63] based on the IoT (Internet of Things) devices, such as RFID, WiFi, and millimeter-wave radar, have been proposed. These pioneering studies reduce the deployment cost of liquid identification systems but have the following limitations in identifying the liquids placed in a packet. Due to the occlusion of the packet or other items (*e.g.* books), many excellent but *LoS*

*Corresponding Author

Authors' address: Fei Shang, shf_1998@outlook.com; Panlong Yang, plyang@ustc.edu.cn; Yubo Yan, yuboyan@ustc.edu.cn; Xiang-Yang Li, xi yangli@ustc.edu.cn, CAS Key Laboratory of Wireless-Optical Communications, School of Computer Science and Technology, University of Science and Technology of China , No. 96 Jinzhai Road, Hefei, Anhui, China, 230027.

Permission to make digital or hard copies of all or part of this work for personal or classroom use is granted without fee provided that copies are not made or distributed for profit or commercial advantage and that copies bear this notice and the full citation on the first page. Copyrights for components of this work owned by others than ACM must be honored. Abstracting with credit is permitted. To copy otherwise, or republish, to post on servers or to redistribute to lists, requires prior specific permission and/or a fee. Request permissions from permissions@acm.org.

© 2022 Association for Computing Machinery.

2474-9567/2022/12-ART181 \$15.00

<https://doi.org/10.1145/3569469>

path-based (such as camera-based) or contact-based methods are no longer applicable. For example, CapCam [67] uses the smartphone's camera to capture the ripples when the liquid vibrates to identify the liquid. But many packets are opaque, which makes it difficult for us to capture the ripples of the liquid through the camera. Vi-Liquid [26] uses a smartphone attached to the container to obtain viscosity to identify liquids, which is difficult to deploy for in-packet liquid identification. TagTag [63], RF-EATS [24], mSense [60], FG-LiquID [37], and OSL [59] use RFID or millimeter wave radar to obtain the signal reflected on the surface of the material to identify the liquid. For a bottle of liquid placed in the packet, it is not easy to obtain the signal reflected by the container. TagScan [58], LiquID [15], and WiMi [19] analyze the changes in amplitude and phase after the signal is transmitted through the dielectric to complete the material identification. These methods have the opportunity to achieve non-contact liquid sensing in the context of NLoS, but they *require prior knowledge* (e.g. material and width of the container) of the channel, which is difficult to satisfy because *the relative position of the items in the packet and the information of the container (material, shape, etc.) are complex and changeable. Furthermore, none of these works take into account the height change of the liquid*. However, both being consumed and the container tilted will cause the liquid height to change.

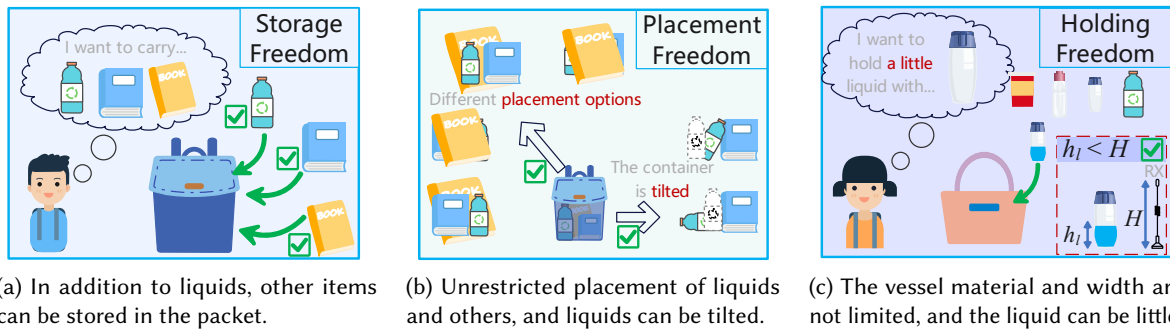


Fig. 1. The three goals that the system needs to achieve: storage freedom, placement freedom, and holding freedom.

In this paper, we propose *PackquID*, a ubiquitous RF system capable of identifying the liquid inside the packet. Specifically, *PackquID* has three desirable priorities:

- *Storage freedom*. Different people have different travel purposes or multiple preferences for different packets, which means that the packets used to store cups (or drink bottles) are diverse. On the other hand, besides the container, people usually place some other items (e.g. books and clothes) inside the packet. *PackquID* is able to identify liquids without being affected by the packet and other items.
- *Placement freedom*. Everyone has their own placement habits, which makes the placement of items in the packet vary from person to person. In addition, the container placed in the packet may be tilted, which increases the number of placement situations. *PackquID* can accurately identify liquids in different situations.
- *Liquid freedom*. On the one hand, different people prefer different containers, which makes for a wide variety of containers that are used to hold liquids. On the other hand, the liquid height will be changed when the liquid is drunk. And *PackquID* manages to identify the liquid independent of the container and liquid height.

PackquID's feasibility for liquid identification stems from that wireless signals are attenuated differently in different liquids [20, 29, 52]. We can use the *attenuation factor* of the liquid to construct features for recognizing the liquids. However, there are three challenges that need to be solved first.

(1) *Unable to tell if the signal contains liquid information.* Since we do not restrict the relative position of the liquid in the backpack to other items (**placement freedom**), it is difficult to determine where the transmitting and receiving antennas are placed so that the RF signal will pass through the liquid.

(2) *Other items interfere with the extraction of liquid features.* In an RF link, the strength of the received signal is affected by many factors, including the type of dielectric, the transmission distance, the degree of refraction on the interface of different dielectrics, and *etc.* [20, 28, 29, 34, 55] However, since we do not know in advance what (*e.g.* containers, books, *etc.*) is put in the packet (**storage freedom**) and how they are placed, the transmission distance of the signal in the liquid (the width of the container), the degree of refraction in the transmission process and the degree of attenuation in other items are unknown, which makes it is difficult to directly compute the value of the attenuation factor.

(3) *Liquid height affects feature extraction.* Conventional wireless channel models (*e.g.* CSI model [62]) may need the liquid is higher than the antennas for liquid recognition. Otherwise, only a portion of the electromagnetic wave reaching the receiving antenna passes through the dielectric, which makes the strength of the received signal related to the height of the dielectric. As a result, the liquid feature constructed with signal attenuation will vary with liquid height. However, both the liquid being drunk and the tilting of the container will cause a change in the height of the liquid. For **holding freedom**, we need to remove the signal difference due to the change in height, but the height of the liquid and the antennas are all unknown to us.

Our solutions. The key idea comes from the fact that the complex permittivity of different dielectrics has different trends with frequency.

Firstly, based on the attenuation factor, we build an RF-based dual antenna model (Sec. 5.1), which help us remove the influence of factors (such as the antenna gain) independent of transmission distance. Noting that the attenuation factors of solids varies less with frequency than that of liquids [8, 9, 35], we calculate the difference in amplitude of signals at different frequencies to identify whether the signal passed through the liquid (Sec. 5.2).

Secondly, since the attenuation factor of the solid varies very little with frequency, we use the method of differential signal difference of different frequencies to eliminate the influence of other items. Benefiting from the fact that the attenuation factor of the liquid varies significantly with frequency [32, 33], we extract the relative value of the attenuation factors from the signal at multiple frequencies, which is independent of the container width. Based on the above two points, we construct the *relative frequency response factor* as a feature to identify the liquid (Sec. 5.3).

Thirdly, to remove the effect of height, we model the transmit and receive antennas as thin straight antennas instead of a point. Combining the distribution of the electric field in space, we extend the model to establish a functional relationship between the received signal strength and the dielectric height (Sec. 5.4). When the transmitting antenna is moved a small distance, the electric field below the liquid level will change. We extend the dual antenna model so that it can use this difference to extract the relative frequency response factor. In summary, we build a model-driven system to identify the liquid in the packet.

Contributions: The main contributions in *PackquID* summarise as follows:

- We design *PackquID*, which can identify the type of liquid in a packet even if the material and width of the packet, the type and placement of the items in the packet, the material and width of the container, and the height of the liquid are all unknown.
- We build a dual-antenna model to remove the influence of factors independent of transmission distance. Using the characteristic that the attenuation factor of liquids varies more with frequency than that of solids, we devise a method to discriminate whether a liquid passes through the liquid, and construct the relative frequency response factor as the liquid feature, which is independent of the transmission channel. Using the electric field difference when the spatial position of the transmitting antenna changes, we extend our

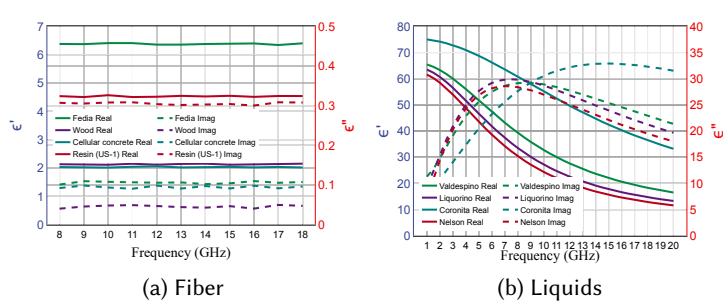


Fig. 2. The complex permittivity of liquids varies significantly with frequency, but solids (e.g. fibers) do not.

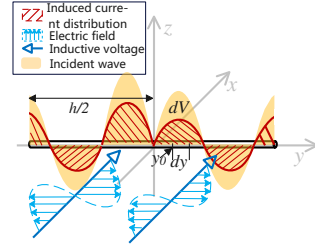


Fig. 3. The induced voltage is the integral of product of induced current and the field strength over the receiving antenna.

model from 2D to 3D, which allows *PackquID* to recognize the liquid independently of the height of the liquid and the antennas.

- We test *PackquID* on 9 common beverages, and the accuracy rate of liquid recognition is more than 99.25%. In Sec. 6.2.2 we conduct the tests on storage freedom. We use 4 different kinds of packets and put clothes, books, etc. in the packet, and *PackquID* still has an accuracy of more than 89% in identifying liquids. In Sec. 6.2.3 we conduct the tests on placement freedom. When the position of the items in the packet are different, and the container types are different (5 types are tested). In Sec. 6.2.4 we conduct the tests on holding freedom. When the liquid height changes from 4 cm to 12 cm, the average accuracy of liquid recognition exceeds 87%.

The rest of the paper is organized as follows. In Section 2, we present the background of the attenuation factor, complex permittivity, and antenna. In Section 4, we introduce the components of our system. We detail how to identify whether the signal has passed through the liquid, the method of obtaining liquid features, and how to identify liquids without being affected by the height in Section 5. In Section 6, we present several case studies to evaluate our system. We discuss the related work in Section 7.

2 PRELIMINARIES

2.1 Attenuation Factor

The energy of electromagnetic waves attenuates when traveling through a dielectric. We use the attenuation factor, α , which is defined as the width of the material needed to decay the strength of the electromagnetic field to $1/e = 0.368$ of its original value, to describe the attenuation of the electromagnetic field [20].

$$\alpha = \frac{2\pi}{\lambda} \sqrt{\frac{\epsilon'}{2} \left(\sqrt{1 + (\frac{\epsilon''}{\epsilon'})^2} - 1 \right)} \quad (1)$$

where λ is the wavelength of electromagnetic waves in the vacuum. ϵ' and ϵ'' are the real and imaginary parts of the complex permittivity of the liquid, respectively. The attenuation factor depends only on the complex permittivity of the liquid, which can be used to build a feature to identify the liquids (Sec. 5.3).

2.2 The Relationship between Complex Permittivity and Frequency

The value of the permittivity generally depends on the frequency at which the sample is radiated. The relationship between the permittivity and the frequency of a dielectric is related to the polarization properties of the molecule [23]. Suppose there are n_j electrons in a molecule with frequency ω_j and damping γ_j . If there are N molecules per unit volume, then the complex polarization, \tilde{P} , is

$$\tilde{P} = \frac{Nq^2}{m} \mathbf{E} \left(\sum_j \frac{n_j}{\omega_j^2 - \omega^2 - i\gamma_j\omega} \right) \quad (2)$$

As a result, the relative complex permittivity of the dielectric can be expressed as

$$\epsilon_r = 1 + \frac{Nq^2}{m\epsilon_0} \sum_j \frac{n_j}{\omega_j^2 - \omega^2 - i\gamma_j\omega} \quad (3)$$

Common liquids such as water and wine are more polar than paper (vegetable fiber) and cloth. Therefore, when the frequency changes, the complex permittivity of the liquid changes more significantly. With the complex permittivity [4, 8, 11, 39, 65], we calculate the attenuation factors for different liquids and solid media by Equ. 1, and the results are shown in the Fig. 2. Based on this property, we devise a method to discriminate whether the signal passes through the liquid (Sec. 5.2).

2.3 The Relationship between Signal Strength and Electric Field Distribution

Since the attenuation of the electromagnetic wave is different when it transmits in air and other dielectrics (e.g. liquid and books) [7, 27], the difference in dielectrics height will lead to different signal strength. For removing the influence of the height, we need to know the relationship between the signal strength and electric field distribution.

As shown in 3, with an electric field E in the y direction, a linearly polarized plane wave is incident on the antenna from the x direction. On the differential element at y_0 , the induced voltage caused by the incident wave is given by [34, 36, 44]:

$$dV = Ef(y_0)dy \quad (4)$$

where $f(y_0)$ is the value of the induced current on the differential element. As a result, the signal strength is the integral of dV :

$$V = \int_{-h/2}^{h/2} Ef(y)dy \quad (5)$$

where h is the height of the receiving antenna.

Using this integral relationship, we extend our signal model to remove the effect of dielectric height (Sec. 5.4).

3 PRE-EXPERIMENTS

We analyze the effect of different packages, items, containers, and liquids on the signal amplitude. We use a signal generator (KEYSIGHT E857D) and a spectrum analyzer (KEYSIGHT N98938B) to test the effect of different materials. In particular:

- *The degree of attenuation of a signal after passing through a solid does not vary with frequency.* Figure 4a shows the ratio of received signal amplitudes in the presence and absence of an item in the RF link. We find that when the frequency of the signal changes, the attenuation of the signal remains basically the same.
- *Thinner items have less effect (less than 2%) on signal amplitude compared to thicker items such as 500-page printer paper and notebooks.* We believe the reason is that these items are poorly conductive and thin (e.g.

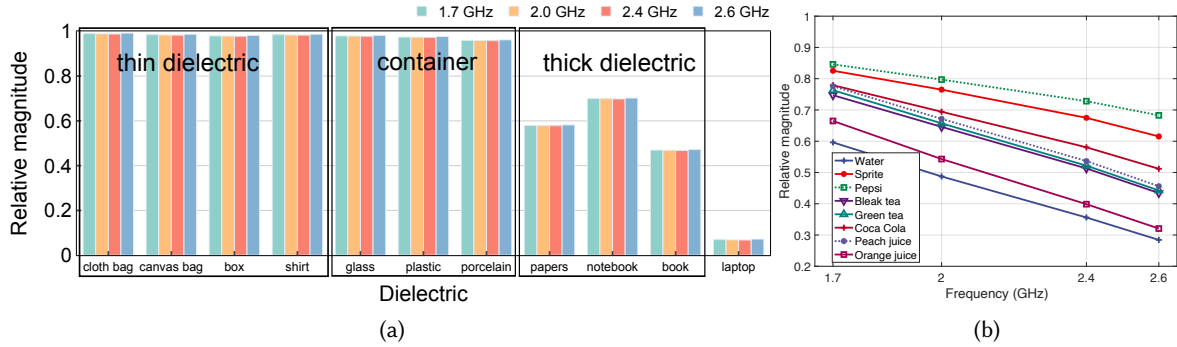


Fig. 4. The effect of different items on signal attenuation. (a) When a signal passes through a solid, the attenuation does not change with frequency. (b) The relative attenuation of different liquids has different trends as a function of frequency.

container walls are typically less than 3 mm). Therefore, we can use the dual antenna ratio method to eliminate their effects.

- When the frequency is changed, the change trend of the signal attenuation in different liquids is different. We use a plastic container with a width of 4 cm to hold the liquid. We test 8 common beverages. The results are shown in Fig. 4b. We find that different liquids have different changes in the decay trend, which gives us the opportunity to distinguish different liquids.
- In addition, our signal is severely attenuated when passing through metal. We test it with a laptop (Surface pro 8), and the amplitude of the signal after passing through the laptop is less than 1/15 of the original. This makes our system not work well when there is a laptop in the backpack or the container is metal.

4 OVERVIEW

We use a transmitting antenna that can move up and down and two receiving antennas of the same model to form a wireless transmission system to identify liquids. The flow chart of the system work is shown in Fig 5. For a packet to be tested, we first need to determine where the liquid is. We divide the packet into M distinct regions and then look for the regions most likely to have liquid. Since we don't know the height of liquids and other items and whether the container is tilted, we first remove the effects of height and tilt after receiving the signals. For signals that contain liquid information and are independent of height, we extract relative attenuation factors as features to identify liquids.

For the convenience of description, we start with the basic situation without considering the liquid height, establish the signal transmission model (Sec. 5.1), the method to detect the liquid position (Sec. 5.2) and how to construct the features only related to the liquid (Sec. 5.3). We then extend the transmission model to make it independent of height by analyzing the distribution of the electric field (Sec. 5.4). At the end, we present the details of our data preprocessing (Sec. 5.5).

Liquid position detection. The intensity of the received signal is affected refraction at the interface of different dielectrics, signal attenuation in dielectrics, and device effects. But some factors have nothing to do with the transmission distance (such as the gain of the antenna), we combine the two antenna signals to remove them (Sec. 5.1). In order to identify whether the received signal has passed through the liquid, we divide the placement of the items and liquid into two cases according to the relative positional relationship. Noting the fact that the attenuation factor of liquids varies more with frequency than that of solids, we emit electromagnetic waves

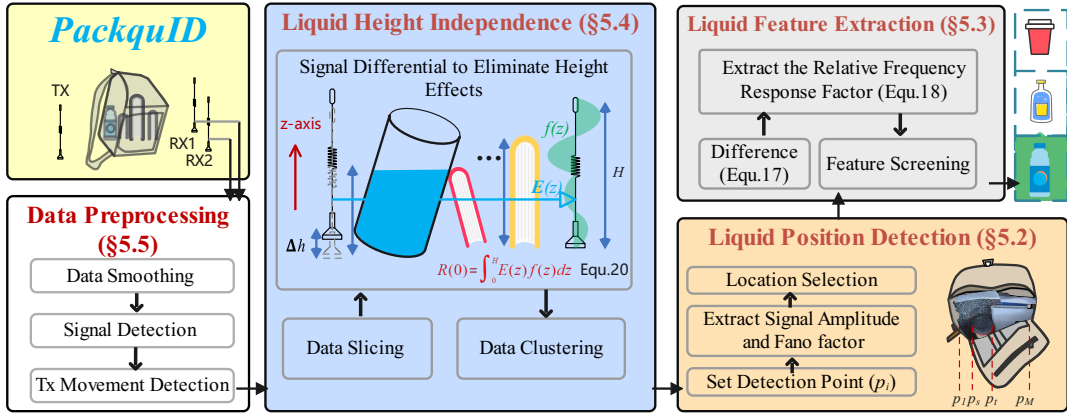


Fig. 5. Overview of the system.

of different frequencies and calculate the Fano factor [17] of the signal strength with respect to frequency to determine whether the signal has passed through the liquid (Sec. 5.2).

Liquid feature extraction. Benefiting from the fact that the attenuation factor of solids varies slowly with frequency, we use the differential of signals at different frequencies to eliminate the attenuation caused by solid dielectrics in RF links. Benefiting from the fact that the attenuation factor of the liquid varies significantly with frequency, we construct the relative frequency response factor as a feature to identify the liquid, which is independent of the width of the container (Sec. 5.3).

Liquid height independence. We construct an electric field distribution model and control the transmitting antenna to rise a certain distance with a motor. Having sliced the data, we use the difference in the electric field caused by the displacement of the transmitting antenna to remove the effect of the height (Sec. 5.4).

Data preprocessing. We process the data collected from the two receiving antennas separately. The data is first filtered and smoothed to suppress noise signals such as thermal noise. Then the signal detection is performed to determine the time when antennas have been placed. Then a segment of the signal is intercepted to recognize the liquid.

5 SYSTEM DESIGN

5.1 Signal Transmission Model

For extracting the attenuation factor information from the signal strength to identify the liquids, we establish a transmission model of the signal.

Fig. 6a shows an RF signal passing through a packet that contains liquids and other items (e.g. books). In the process of transmission, *there are three factors affect signal strength*:

- *Transmission loss in dielectric transmission.* As the distance the signal travels in a dielectric (such as liquid) increases, the signal strength decreases, and the rate of attenuation can be described by the attenuation factor, α .
- *Refraction loss.* When electromagnetic waves are transmitted to the interface of two different dielectric (such as air and packet), they will be refracted and reflected, and part of this energy can be transmitted to the new dielectric [21, 41, 43], which can be described by transmission coefficient, γ .
- *Equipment factors,* such as the gain of the antenna and AGC (automatic gain control).

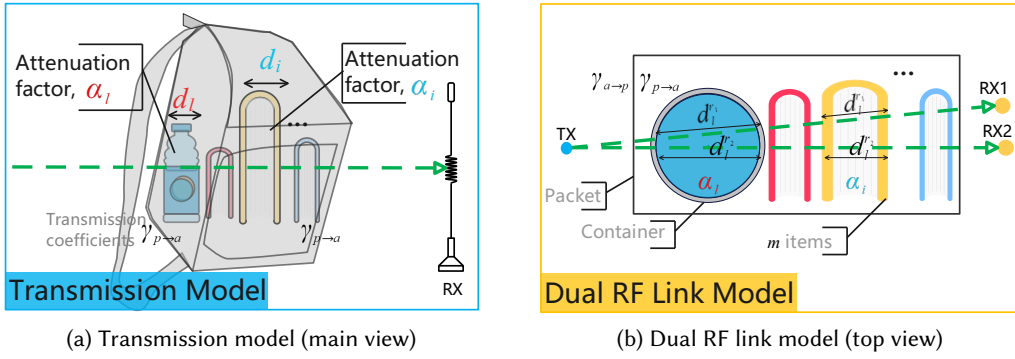


Fig. 6. Basic model of signal transmission.

Basic model. As a result, when we send a signal with strength R_0 , The strength of the received signal is given by [15, 30]:

$$R = g(D) \exp(-\alpha_l d_l) \prod_{i=1}^n \exp(-\alpha_i d_i) \Gamma P R_0 \quad (6)$$

where $g(D)$ is the attenuation of electromagnetic waves in the air with the transmission distance. α_l and d_l are the attenuation factor of liquid and the transmission distance in the liquid, respectively. α_i and d_i are the attenuation factor of the i -th solid dielectric and the transmission distance in this dielectric, respectively. Γ is the product of the transmission coefficients across the interfaces, including the air-packet interfaces ($\gamma_{a \rightarrow q}$, $\gamma_{q \rightarrow a}$), the air-container interfaces ($\gamma_{a \rightarrow c}$, $\gamma_{c \rightarrow a}$), and etc. n is the number of solid dielectrics. And P is the factor caused by equipments.

Dual RF link model. Noting that many of the variables (e.g. Γ) in Equ. 6 are independent of the signal transmission distance, we remove their effects using a two-antenna model. Similar to the basic model, as shown in Fig. 6b when we use two RF links simultaneously, the signal strengths received by the two receive antennas are:

$$\begin{aligned} R_{r1} &= g(D_1) \exp(-\alpha_l d_l^{r1}) \prod_{i=1}^n \exp(-\alpha_i d_i^{r1}) \Gamma P R_0 \\ R_{r2} &= g(D_2) \exp(-\alpha_l d_l^{r2}) \prod_{i=1}^n \exp(-\alpha_i d_i^{r2}) \Gamma P R_0 \end{aligned} \quad (7)$$

where D_1 and D_2 are the transmission distances in the air of the two RF links, d_l^{r1} and d_l^{r2} are transmission distances in the i -th solid dielectric of the two RF links.

Model analysis. Because the distance (more than 30 cm) between the transmitting and receiving antennas is much larger than the distance between the two receiving antennas, we approximately think that $D_1 \approx D_2$. Since the dielectric interface and types of the equipment are the same for both links, the Γ and P are respectively the same. In addition, we notice that the thickness of some solid dielectrics (such as container wall and packet shell) is usually less than 3 mm. For these dielectrics, we think that $d_i^{r1} \approx d_i^{r2}$. As a result, we can remove these same factors:

$$\Delta R = \frac{R_{r1}}{R_{r2}} = \exp(-\alpha_l \Delta d_l) \prod_{i=1}^m \exp(-\alpha_i \Delta d_i) \quad (8)$$

where $\Delta d_l = d_l^{r1} - d_l^{r2}$ and $\Delta d_i = d_i^{r1} - d_i^{r2}$ and m is the number of thick solid dielectrics.

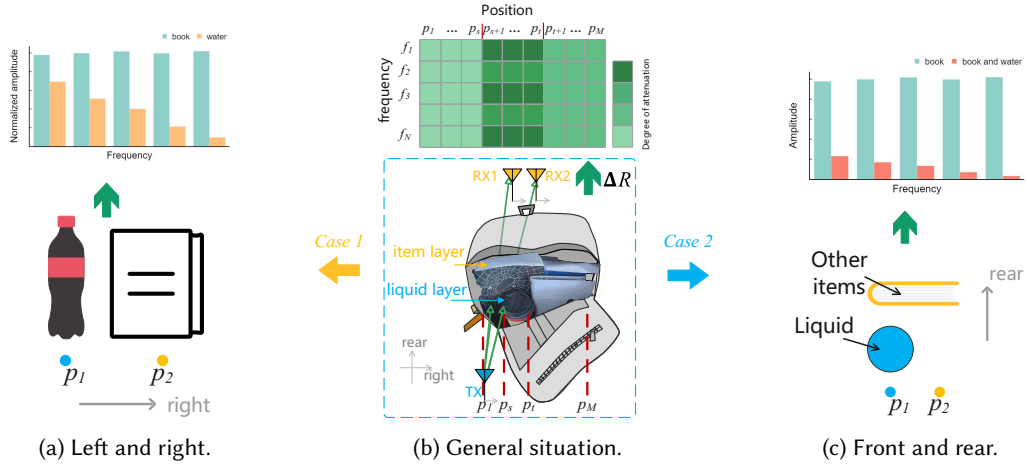


Fig. 7. The relative position of the liquid to other items.

5.2 Liquid Position Detection

We use a system of one transmitting and two receiving antennas to identify liquids. But since many packets are opaque, we don't know where the liquid is placed. For liquid identification, when we receive an RF signal, we first need to determine whether the signal contains liquid information.

Basic idea. Typically, in a packet, there are other items such as books and notebooks to the right (or left) and back (or front) of the liquid. As shown in Fig. 7, we classify the relative positions of liquids and other items into two cases and propose methods to extract signals with liquid information respectively.

- (1) *Left and right.* As shown in Fig. 7a, we sometimes pack liquids and other items (e.g. books) side by side. Without loss of generality, we assume that the liquid is on the left and other items are on the right. Since the changing trend of the attenuation factor of liquid with frequency is more obvious than that of solid, we use the difference of different frequency signals to obtain signals through the liquid.
- (2) *Front and rear.* As shown in Fig. 7c, Sometimes larger items (e.g. notebooks) and liquids are placed one in the front and one in the rear. Without loss of generality, we assume that the liquid is on the front. The amplitude of the signal containing the information in the liquid (left) is smaller than that without (right) due to the energy attenuation of the signal as it travels through the liquid, which makes it easy to distinguish whether the signal has passed through the liquid.

Case 1: Left and right. When we send a signal with the frequency of f_i , according to Equ. 8, the relative strength of the received signal with liquid information on the left ($\Delta R_{p_1}^{f_i}$) and without liquid information on the right ($\Delta R_{p_2}^{f_i}$) are respectively by:

$$\begin{aligned}\Delta R_{p_1}^{f_i} &= \exp(-\alpha_l^{f_i} \Delta d_l) \\ \Delta R_{p_2}^{f_i} &= \prod_{i=1}^m \exp(-\alpha_i^{f_i} \Delta d_i)\end{aligned}\tag{9}$$

where α is the attenuation factor, Δd is the distance difference between two RF links, and m is the number of items.

Having sent N different frequencies, $[f_1, \dots, f_N]$, we get two sets of signal strengths:

$$\begin{aligned} S_{p1} &= [\Delta R_{p1}^{f_1}, \Delta R_{p1}^{f_2}, \dots, \Delta R_{p1}^{f_N}] \\ S_{p2} &= [\Delta R_{p2}^{f_1}, \Delta R_{p2}^{f_2}, \dots, \Delta R_{p2}^{f_N}] \end{aligned} \quad (10)$$

We distinguish the two sets by the magnitude of the **Fano factor** [17], which is defined as $W = \frac{\sigma^2}{\mu}$, where σ is the standard deviation of S_p , and μ is the mean of the S_p . Fig. 7a shows the difference in the Fano factor between these two types of sets. For the actual measurement, we run the packet across the RF links from left to right. Using the pigeonhole principle [2], for a packet of width L_p and a container of length L_c , we set a total of M positions, where

$$M = \lfloor \frac{L_p}{L_c} \rfloor + 1 \quad (11)$$

In these positions, we collect signals and calculate their Fano factors, $[W_{p1}, \dots, W_{pM}]$. The position with the largest Fano factor is taken as the position of the liquid. As a result, the signal set with liquid information can be given by:

$$\begin{aligned} S_l &= [\Delta R_l^{f_1}, \Delta R_l^{f_2}, \dots, \Delta R_l^{f_N}] \\ &= [\Delta R_{pi}^{f_1}, \Delta R_{pi}^{f_2}, \dots, \Delta R_{pi}^{f_N}], \text{ where } W_{pi} = \max\{W_{p1}, W_{p2}, \dots, W_{pM}\} \end{aligned} \quad (12)$$

Case 2: Front and rear. As shown in Fig. 7c, when we send a signal with frequency of f_i , according to Equ. 8, The relative strength of the received signal with liquid information on the front ($\Delta R_{p1}^{f_i}$) and without liquid information on the rear ($\Delta R_{p2}^{f_i}$) are respectively by:

$$\begin{aligned} \Delta R_{p1}^{f_i} &= \exp(-\alpha_l^{f_i} \Delta d_l) \prod_{i=1}^m \exp(-\alpha_i^{f_i} \Delta d_i) \\ \Delta R_{p2}^{f_i} &= \prod_{i=1}^m \exp(-\alpha_i^{f_i} \Delta d_i) \end{aligned} \quad (13)$$

where α is the attenuation factor, Δd is the distance difference between two RF links, and m is the number of items.

$\Delta R_{p1}^{f_i}$ is more attenuated than $\Delta R_{p2}^{f_i}$, which helps us determine whether the signal has passed through the liquid. Similar to the *case 1*, we set M (Equ. 11) different positions to get signals. For a frequency of f_i , we think the signal at the position, where the signal strength is smallest, passes through the liquid. For each frequency, we calculate the position with the smallest signal strengths. And at the position with the most occurrences in the results, the signal is considered to have passed through the liquid.

General situation. The more general case is that there are items around the liquid, we treat it as a combination of *case 1* and *case 2*. As shown in Fig. 7b, we use the pigeonhole principle to set M (Equ. 11) positions, first use the difference in relative strength (ΔR) to exclude the positions (from p_1 to p_s in Fig. 7b) where liquid layer has no items. Then, we use the difference in Fano factors (W) to select the positions (from p_t to p_M in Fig. 7b) where liquid layer has items. At this area, with N frequencies, the relative strength set, S_l , which is used to identify the liquid is:

$$S_l = [\Delta R_l^{f_1}, \Delta R_l^{f_2}, \dots, \Delta R_l^{f_N}], \quad (14)$$

where

$$\Delta R_l^{f_i} = \exp(-\alpha_l^{f_i} \Delta d_l) \prod_{i=1}^m \exp(-\alpha_i^{f_i} \Delta d_i) \quad (15)$$

In this way we can determine the location of the liquid in the packet, which makes liquid identification independent of the relative position of the container and other items. As a result, we realize placement freedom. We validate it in the Sec. 6.2.3.

5.3 Liquid Feature Extraction

As shown in Equ. 15, we obtain the relative signal strength, $\Delta R_l^{f_i}$, which contains the liquid information. We need to build a feature to distinguish different liquids, but it is difficult to directly extract the attenuation factor, α_l . Based on the property that the attenuation factor varies with frequency, we design the *relative frequency response factor* as a feature to help us identify liquids.

The challenge of extracting the attenuation factor comes from two aspects:

- *The unknown width of the container makes the system of equations underdetermined.* As shown in Equ. 8, the attenuation factor α_l and the container width Δd_l are coupled together. If there are k different RF links in the environment to construct k sets of equations, then there are k unknown variables Δd_l and the attenuation factor α_l , for a total of $k + 1$ unknowns. This is an underdetermined system of equations that cannot have a unique solution.
- *Interference from solid items.* As shown in Equ. 8, the relative signal strength (ΔR_l) is affected by both liquids and other solid items. But to us, the quantity (m) and material (affecting the attenuation factor α_i) of other items, and the relative transmission distance (Δd_i) of the signal in these items are unknown.

Opportunities from attenuation factor variation with frequency:

- (1) Extract the relative value of the attenuation factor. Although the signals of different frequencies can't help us obtain a system of positive definite equations, they give us an opportunity to obtain the relative values of attenuation factors. Since the attenuation factor is different when the frequency is different [8, 20, 31, 50, 57], for the same RF link, we transmit N different frequency signals, and we build a system of equations with N different attenuation factors and one unknown container width, which make it is possible to obtain a set of relative solutions.
- (2) Eliminate "static" disturbances caused by solids with differential. The attenuation factor of solids varies little with frequency while the attenuation factor of liquids varies significantly, which allows us to treat the attenuation caused by solids as a static variable when frequency changes. This static variable can be eliminated by using differences in relative signal strengths obtained at different frequencies.

Extract the relative frequency response factor. The attenuation factor of solid is stable with frequency, as a result, we denote the attenuation factor of the i -th solid by α_i :

$$\alpha_i = \alpha_i^{f_1} = \dots = \alpha_i^{f_N} \quad (16)$$

With two RF links and N signals of different frequencies, we can get a set of relative signal strengths containing the liquid information, $S_l = [\Delta R_l^{f_1}, \Delta R_l^{f_2}, \dots, \Delta R_l^{f_N}]$, which is described by Equ. 15. When $p \neq q$,

$$\begin{aligned} \Delta R_l^{f_p} &= \exp(-\alpha_l^{f_p} \Delta d_l) \prod_{i=1}^m \exp(-\alpha_i \Delta d_i) \\ \Delta R_l^{f_q} &= \exp(-\alpha_l^{f_q} \Delta d_l) \prod_{i=1}^m \exp(-\alpha_i \Delta d_i) \end{aligned} \quad (17)$$

As a result, we can get an equation independent of Δd :

$$J_{p,q} = \frac{\Delta R_l^{f_p}}{\Delta R_l^{f_q}} = \exp[-(\alpha_l^{f_p} - \alpha_l^{f_q})\Delta d_l] \quad (18)$$

For $(p, q) \neq (u, v)$,

$$K_{u,v}^{p,q} = \frac{\ln(J_{p,q})}{\ln(J_{u,v})} = \frac{\alpha_l^{f_p} - \alpha_l^{f_q}}{\alpha_l^{f_u} - \alpha_l^{f_v}} \quad (19)$$

When p, q, u, v change from N to 1, we can get the **relative frequency response factor** $F = [K_{N,N-2}^{N,N-1}, K_{N,N-3}^{N,N-1}, \dots, K_{2,1}^{3,1}]$, whose dimensions are $\binom{N}{2}$, where $\binom{n}{k} = \frac{n!}{(n-k)!k!}$.

Feature Screening. We use electromagnetic waves in four frequency bands 4.8 GHz, 5.1 GHz, 5.4 GHz, and 5.7 GHz, so a 15-dimensional feature can be extracted. We are using 8 different liquids, including Pepsi, Master Kong Ice Black Tea (a tea beverage), Coca-Cola, Master Kong Green Tea (a tea beverage), orange juice, peach juice, water, and Sprite as the test solution to collect 50 sets of data independently. Then calculate the variance of each dimension feature. For us, the dimension with better stability is selected as the final liquid feature.

As a result, we can extract the liquid feature without being affected by packet material and other items, which means we achieve storage freedom for liquid identification. We describe the tests associated with it in Sec. 6.2.2.

5.4 Liquid Height Independence

In previous sections, we introduce methods for identifying liquids using RF signals to construct relative frequency response factors. However, it is not applicable to the situation where liquid or solid items are below the antennas. The reason is that the total induced voltage strength on the receiving antenna is related to the surrounding electric field distribution, and the height of the liquid or solid items will affect the electric field distribution. In order to eliminate the influence of height, we build a model of the electric field distribution in space. With the electric field change caused by the displacement of the transmitting antenna, we extract the relative intensity independent of height, which extends the applicability of our model from 2D to 3D.

The difference in height causes the difference in the distance that the signal travels in the dielectrics, which causes the difference in the distribution of the electric field around the antenna. Without loss of generality, we define the z -axis to be parallel to the antenna. At this time, the transmission distance of the signal in liquid and i -th solid item is represented by two functions related to z , $d_l(z)$ and $d_i(z)$, respectively. There are two situations in which the height of the dielectric affects the transmission distance:

- *Liquid dielectric.* As shown in the left part of Fig. 8, the height of the liquid contained in an inclined container is smaller than that of the antenna. There are three cases for the value of signal transmission distance, $d_l(z)$. (i) 0. In the part where there is no liquid (above the dashed line c), the signal is equivalent to passing through a liquid of width 0. (ii) d_l^0 . Between the dashed lines b and c, the distance the signal travels in the liquid is a z -independent value, d_l^0 , which depends on the container width and inclination angle. (iii) d_l^z . In the part where the liquid level is inclined (for example, between the dotted lines a and b), the transmission distance of the signal varies with z .
- *Solid dielectric.* The right part of Fig. 8 shows the situation of the i -th solid dielectric contained. There are two cases for the value of signal transmission distance, $d_i(z)$. (i) 0. In the part where there is air (above the dashed line b), the signal is equivalent to passing through a solid dielectric of width 0. (ii) d_i^0 . Between the dashed lines a and b, the distance the signal travels is a z -independent value, d_i^0 , which depends on the solid width and its inclination.

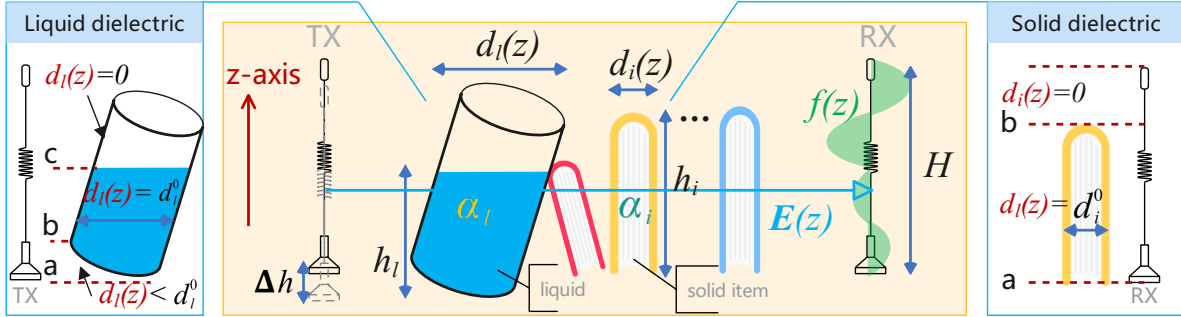


Fig. 8. Height model.

Distribution model of the electric field. As shown in Fig. 8, similar to Equ. 8, the transmitting antenna emits a beam of electromagnetic waves with an electric field strength E_0 at z , then when the electromagnetic wave reaches the receiving antenna, the electric field strength $E(z)$ is given by:

$$E(z) = g(D) \exp(-\alpha_l d_l(z)) \prod_{i=1}^M \exp(-\alpha_i d_i(z)) \Gamma P E_0 \quad (20)$$

where $g(D)$ is the transmission distance of the signal in air, $d_l(z)$ is the distance the signal travels in liquid, $d_i(z)$ is the distance the signal travels in solid, α_l is the attenuation coefficient of liquid, α_i is the attenuation coefficient of i -th solid dielectric, M is the number of solid dielectrics, P is the impact of equipment, and Γ is the product of the transmission coefficients across the interfaces.

Signal transmission model in 3D. The received signal strength R can be regarded as the integral of the induced voltage on the antenna. Assuming that the magnitude of the induced voltage is proportional to the induced current and the electric field is distributed in the plane 0 and $z = H$ directly, we can get:

$$R(0) = \int_0^H E(z) f(z) dz \quad (21)$$

where $f(z)$ is the distribution of induced current on the antenna, which is related to the type of antenna and the wavelength of the signal, and H is the height of the antenna.

Signal differential to eliminate height effects. When z_0 is less than the height h_l of the liquid, the transmission distance of the signal in the liquid varies continuously with z_0 . For a differentiator Δh , we approximate that $d_l(z_0 + \Delta h) = d_l(z_0)$. Similarly, for the i -th solid dielectric, $d_i(z_0 + \Delta h) = d_i(z_0)$. When the transmitting antenna is displaced upward by z_0 , the electric field is distributed in the plane $z = 0$ and $z = H$ directly, we can get:

$$R(z_0) = \int_{z_0}^H E(z) f(z) dz \quad (22)$$

and

$$\begin{aligned} dR(z_0) &= R(z_0 + \Delta h) - R(z_0) = \int_{z_0}^{z_0 + \Delta h} E(z) f(z) dz \\ &= g(D) \exp(-\alpha_l d_l(z_0)) \prod_{i=1}^M \exp(-\alpha_i d_i(z_0)) \Gamma P E_0 \Delta h \end{aligned} \quad (23)$$

When we consider two RF links,

$$\begin{aligned} dR_{r1}(z_0) &= g(D_1) \exp(-\alpha_l^{r1} d_l(z_0)) \prod_{i=1}^M \exp(-\alpha_i^{r1} d_i(z_0)) \Gamma P E_0 \Delta h \\ dR_{r2}(z_0) &= g(D_2) \exp(-\alpha_l^{r2} d_l(z_0)) \prod_{i=1}^M \exp(-\alpha_i^{r2} d_i(z_0)) \Gamma P E_0 \Delta h \end{aligned} \quad (24)$$

When we consider the ratio of the two RF links,

$$\Delta R = \frac{dR_{r1}(z_0)}{dR_{r2}(z_0)} = \exp(-\alpha_l \Delta d_l) \prod_{i=1}^m \exp(-\alpha_i \Delta d_i) \quad (25)$$

which has the same form as Equ. 8. In this way, we can use this result to proceed with liquid position detection (Sec. 5.2) and liquid feature extraction (Sec. 5.3). As a result, we extend the original 2D model to 3D, and it is compatible with the previous methods.

Slicing and Clustering. As shown in Equ. 25, we only need the data of two adjacent positions to calculate the fingerprint of the liquid. However, due to the existence of random noise and other factors, Δa may not be able to perform subsequent processing (such as Δa is a negative value). We devise some methods to avoid this. For each frequency of data, we randomly compute a slice (width is 1000 samples). For those slices, we fit a 5th order polynomial to the data and use them to calculate relative attenuation factors. We cluster the attenuation factors for each dimension (choose 0.2 for the inter-class distance) [47]. Then check if the number of samples in the largest class exceeds 50% of the total. If the number of dimensions satisfying the condition is less than 3, we re-slice the signal. By screening multiple times, we have a greater probability of obtaining stable data. Although theoretically the transmitting antenna (TX) only needs a small displacement (Δh) to eliminate the effect of height, due to factors such as random noise and sampling error, we make the TX rise at least 2 cm during the test to ensure that we have enough data to select data slice.

We extend the signal transmission model to remove the effect of height, which allows *PackquID* to perform accurate liquid identification without presenting the height of the liquid in the container to achieve holding freedom. We conduct related tests in Sec. 6.2.4.

We construct the basic transmission model of the signal in the 3D range, use the change of the attenuation factor with frequency to identify whether the signal contains liquid information, and construct the relative frequency response factor as a feature to identify the liquid.

5.5 Data Preprocessing

Data smoothing. After the liquid is present in the RF link, the amplitude of the signal is significantly attenuated. Factors such as thermal noise of the device make a lot of Gaussian noise superimposed on the received signal. To suppress the effect of noise, we smooth the data using a Gaussian window of width 1000.

Signal extraction. After smoothing the amplitude curve, we apply a sliding window to continuously detect if the packet to be tested is present in the RF link. The variance of the amplitude value in the sliding window reflects the degree of amplitude fluctuation. When the variance is large and the amplitude is decreasing, we consider a packet to be placed in the RF link; when the variance is large and the amplitude is increasing, we consider a liquid to be taken out of the RF link.

Tx movement detection. During the high correction stage, the signals consist of a three-stage process: the transmitting antenna is stationary; the transmitting antenna is moved upward; the transmitting antenna is stationary. To identify the liquids, we need to determine when the transmit antenna starts to rise. As shown in Fig. 9, we use the double sliding windows detection algorithm to detect the start point of the signal, which is

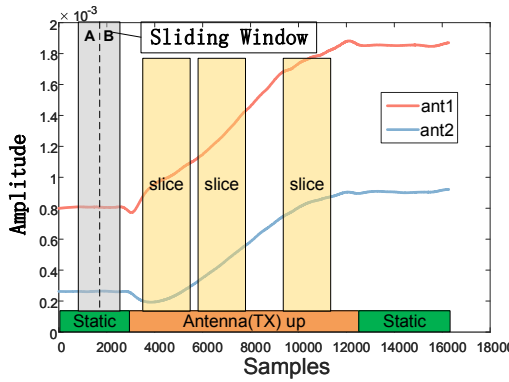


Fig. 9. Sliding window detection and data slicing.

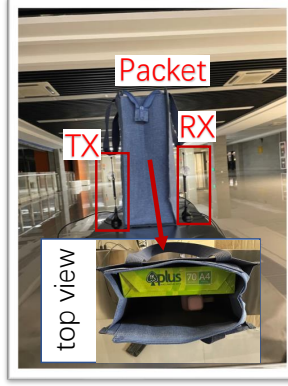


Fig. 10. Experimental setup.



Fig. 11. Bags and vessels.

similar to WiFi's packet detection. We set up two sliding windows A and B, whose width are both L . Then we calculate the ratio of the energies of the signals in the two windows [54]:

$$ra_i = \frac{\sum_{m=0}^{L-1} r_{i-m} r_{i-m}^*}{\sum_{l=1}^L r_{i+l} r_{i+l}^*} \quad (26)$$

where r is the amplitude of the signal, and r^* is the conjugate of r , and i is the right edge of window A. When the window slides from left to right, for a signal series of length N , we obtain the set $Ra = [ra_{L-1}, \dots, ra_{N-L-1}]$, and then we compute the difference of Ra , $Dra = \text{diff}(Ra)$. Because the signal amplitude in the stationary phase is relatively stable, when both windows contain only the signal in the static, the value of Dra is small; conversely, when one window only contains the signal in the static and the other window contains the signal in the antenna rising, the value of Dra begins to change rapidly. If the value of Dra at i is greater than 50 times the value of Dra at rest, we consider the antenna to start to rise.

6 EVALUATION

6.1 Experimental Setup

Hardware setup. As shown in Fig. 10, we use an NI company's N2944R USRP to transmit RF signals, and another of the same model to receive signals. The antennas we use can send and receive wireless signals in the frequency range of 1710-2700 MHz and 4900-5850 MHz. We use one transmitting antenna and two receiving antennas, whose gain are 5 dB. We set the ADC sample rate at 40 KHz. We use a 10 G network cable to transfer data from USRP to computer with Intel i7-10700 CPU and 16G memory for processing the RF data.

Experimental Settings. Our experimental setup for evaluating *PackquID* is shown in Fig. 10. We use a transmit antenna and two receive antennas. When collecting data, we place the packet between the receiving antennas and the transmitting antenna. In the process of collecting data, we continue to send a sine signal with a frequency of 4.8 GHz, 5.1 GHz, 5.4 GHz and 5.7 GHz. We send a single-tone IQ signal at 0.8 KHz. Before each experiment, we carefully calibrate the relative positions between the transmitting and receiving antennas. Specifically, the distance between the transmitting and receiving antennas is 30 cm, and the distance between the two receiving antennas is 4 cm.

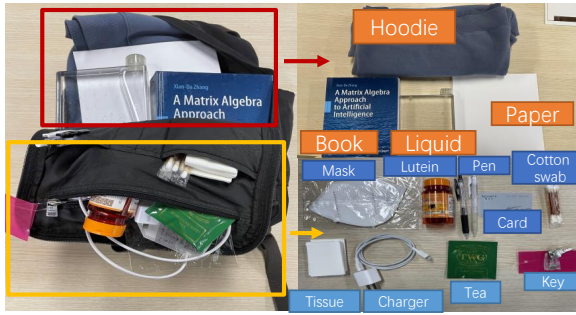


Fig. 12. Liquids, clothes, books and papers in the backpack.

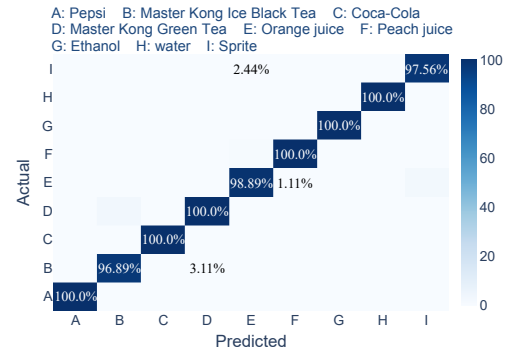


Fig. 13. Identification performance for 9 liquids.

6.2 Micro Benchmark

6.2.1 Basic Experiment.

We first test *PackquID*'s ability to identify liquids.

Recognizing liquid. To verify the effectiveness of our proposed model and techniques, we test 9 common liquids, including Pepsi, Master Kong Ice Black Tea (a tea beverage), Coca-Cola, Master Kong Green Tea (a tea beverage), Orange juice, Peach juice, ethanol, water, and Sprite. All liquids are bought from a supermarket. Similar to RadarCat [66], we collect data samples of 9 different liquids three times a day for three day. For each liquid, we pour 500 ml into a cuboid resin container and place the container on the canvas bag. In order to simulate the normal storage situation, we place 500 pages of A4 size printer paper behind the water cup. For each liquids, we perform 50 independent data collections. The temperature of all liquids is at room temperature between 20°C and 25°C. By taking the relative attenuation factor (using 4 frequencies) as features, we can adopt a simple K-Nearest Neighbors algorithm (K=3) to differentiate those liquids. The identification results are shown in Fig. 13. It achieves an average accuracy of 99.25%. In particular, *PackquID* can accurately distinguish similar liquids including Coke and Pepsi.

Fig. 14 shows how *PackquID* compares with some excellent related work on liquid identification accuracy. *PackquID*'s accuracy is tested in the scenario where the liquid is placed in a backpack, and the backpack also contains a hoodie, a book, and 100 pages of A4 paper (as shown in Fig. 12). We find that these works are similar in terms of liquid identification, but *PackquID* is able to accurately identify liquids with other items in the packet. This is mainly due to the fact that the relative frequency response factor is constructed as a feature by using the characteristic that the complex permittivity of solid and liquid varies with frequency, which eliminates the adverse effects of other items in the packet on liquid identification.

Impact of the number of carriers. We use fine-grained solutions to test the difference of identification ability about different number of carriers. We use 8 common liquids as solvents, including Pepsi, Master Kong Ice Black Tea (a tea beverage), Coca-Cola, Master Kong Green Tea (a tea beverage), orange juice, peach juice, water, and Sprite. For each solvent, we add alcohol to it so that the alcohol concentration varies from 1% to 20% in steps of 1%. We send 4.8 GHz, 5.1 GHz, 5.4 GHz, 5.7 GHz and 2.4 GHz frequency signals respectively, and then use the k-nearest neighbor algorithm (k=1) to identify the concentration. For a single frequency, we use the amplitude ratio of their two receiving antennas as the feature (Equ. 8), and for multiple frequencies, we extract the relative frequency response factor as the feature. We use five-fold cross-validation to test the performance of the system.

The results are shown in Fig. 15. When we use the relative frequency response factor as a feature, the recognition accuracy is significantly improved. This is because different liquids may have similar complex permittivity for a particular frequency. When a signal is transmitted in liquids with similar complex permittivity, the amplitudes are attenuated to a similar degree, making them indistinguishable. However, due to the different polarization

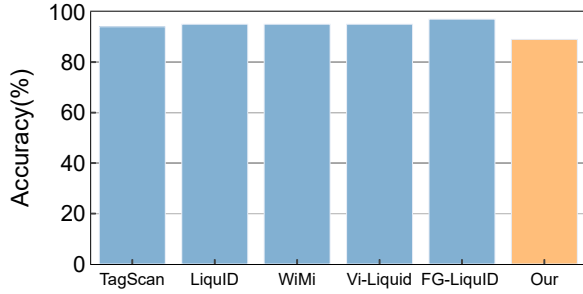
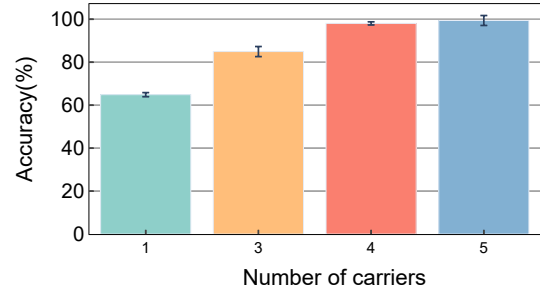
Fig. 14. *PackquID* has similar accuracy to related work.

Fig. 15. Liquid can be identified using four frequencies.

characteristics of different liquid molecules, their complex permittivity changes with frequency in different trends. The relative frequency response factor we constructed with multiple carriers can reflect this trend, which helps us to distinguish different liquids more accurately. Considering the small frequency band range of many antennas, we reduce the frequency separation. We find that 4 frequency points can already realize the recognition liquid, and increasing the number of frequency points will not significantly improve the accuracy. Therefore we choose 4.8 GHz, 5.1 GHz, 5.4 GHz and 5.7 GHz to use.

6.2.2 Identify Liquids with Storage Freedom.

There are two basic requirements for storage freedom:

- (1) Different types of packets can be selected. There are two types of typical packets used to store containers: one is for people to carry around, such as a handbag; the other is for storage or logistics, such as a carton. The packets that people carry with them can be divided into portable and backpack. For these different situations, we select 4 different packets to test, including two handbags, a backpack, and a carton, which are shown in Fig. 11.

- (2) Different items can be placed in the packet. In addition to liquids, the items placed in the packet can be divided into two categories: one is bulky, such as books, clothes and paper, and the other is some scattered small items, such as keys, pens, medicines, instant coffee, and *etc*. We test the accuracy of liquid recognition when the packer contained these items.

Impact of different types of packets. In daily life, we use a variety of packets. To test the impact of different packets, we select 4 common packets with different materials, including the backpack, canvas bag, paper bag, and box for testing, as shown in Fig. 11. For each case, we collect 30 samples of each category shown in Fig. 13. Having obtained the relative attenuation factor (using 4 frequencies) as features, we can adopt a simple K-Nearest Neighbors algorithm ($K=1$) to differentiate those liquids. We use the data of the tested packet as the test set and the data of the other packets to build the classifier. For example, when we test the effect of the backpack on liquid identification, we use data collected with liquid in the backpack as a test set, and data collected with liquids in other packets (canvas bag, paper bags, and box) to build a KNN classifier.

The identification results are shown in Fig. 16. It achieves accuracy over 89.19%. We find that packets of different materials have similar accuracy. This is because that *PackquID* uses the ratio of the two RF signals to extract the liquid feature. The thickness of the packet is usually less than 5 mm. Since the receiving antennas we place are relatively close, for the two RF links, the effect of the packet on them is similar, so the differential method can eliminate the influence of different backpack materials.

Impact of the type of items in the packet. In a more general scenario, the packet contains some other items besides liquids, such as books and clothes. To test *PackquID*'s ability to identify liquid in this situation, we put common items in a backpack, including a water cup, a book, 100 pages of A4 printer paper, a hoodie, and three gel pens. Their placement is shown in the Fig. 12. We test 5 different situations, including a bag with just a water

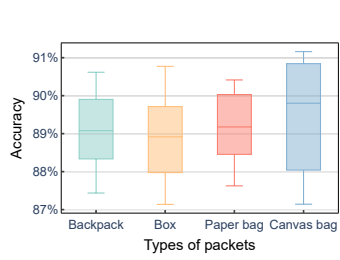


Fig. 16. The impact of different types of packets on identification.

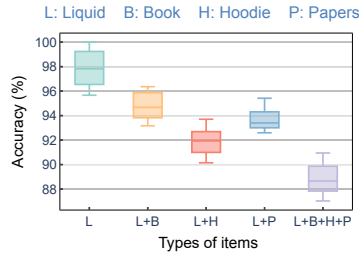


Fig. 17. The impact of different items placed in the packet.

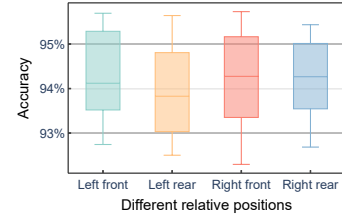


Fig. 18. When the items relative position varies, the accuracy exceeds 90%.

cup, a water cup and a book, a water cup and a hoodie, a book and 100 pages of printer paper, all of them. For the water cup, we use the rectangular water cup shown in D in the Fig. 11. For each situations, we collect data on 9 different common beverages, each beverage collected 30 times independently. Having obtained the relative attenuation factor (using 4 frequencies) as features, we can adopt a simple K-Nearest Neighbors algorithm ($K=1$) to differentiate those liquids. For each test, we use one situation of data as the test set and use other data to build the KNN classifier.

The result is shown in Fig. 17. Even when the bag contains multiple items, the accuracy rate of liquid identification is more than 89%. Furthermore, we find that the accuracy of identification is lower when a hoodie is placed inside the packet than when other items are placed, possibly due to the more uneven surface of the clothing that increased signal scattering compared to books.

6.2.3 Identify Liquids with Placement Freedom. There is a basic requirement for placement freedom: identification is not affected by the location of the container. Specifically, it includes two aspects:

(1) The relative position of the container and other items is different. There are four basic relative positions of the container and other items: the container is in the front left; the container is in the rear left; the container is in the front right; the container is in the rear right. We show these different relative positions in the Fig. 19. To test its ability to perform liquid recognition, we test each of these four different scenarios.

(2) The position of the antenna relative to the container is indeterminate. Since we cannot get the exact location of the container, the position of the antenna relative to the container may be random. As shown in Fig. 20, we divide the area around the container and exhaustively test the ability of *PackquID* to identify liquids when the two receiving antennas are in different positions.

Impact of number of signal acquisition points. Since packets are usually opaque, we don't know where to place the transmitting and receiving antennas to ensure that liquid is present in the RF link. To determine the location of the liquid, as shown in Sec. 5.2, we use the pigeonhole principle to pick M distinct points around the packet. For example, for a packet with a width of 20 cm and a container with a width of 6 cm, we can find the points containing the liquid information as long as we ensure that $M > 3$. The value of the different number of M affects the relative position of the antenna and the container. Due to the large value range of the size of the packet and container in practice, it is difficult for us to test the influence of different values of M on the Identification accuracy in an exhaustive way. Instead, we test the accuracy of the system in identifying liquids when the antenna is in different positions on the container.

The results are shown in Fig. 22, more than 90% accuracy even with different antenna positions. We find that reception is better when the receiving antennas are placed in the middle of the container. We believe this may be due to the fact that antennas are placed in the middle and receive less interference from diffraction and multipath than at the edges. In addition, the accuracy of liquid identification is better when the difference in the

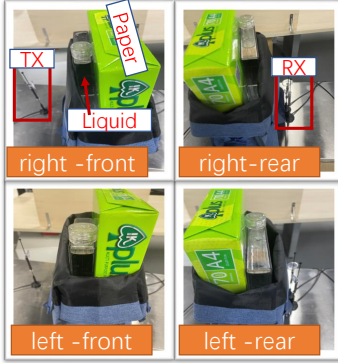


Fig. 19. The relative placement of liquids and other items.



Fig. 20. Different placement of the antenna.

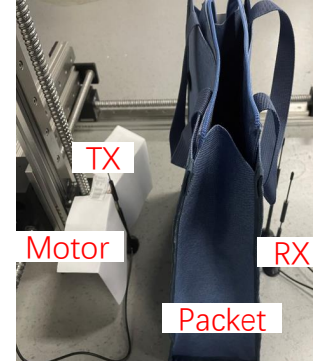


Fig. 21. Use a motor to control the antenna up and down.

transmission distance of the signal for the two RF links in the liquid is large. This is because we extract features from the ratio of the amplitudes of the two RF links to identify the liquids, and the difference in the transmission distance will make the signal ratio larger, which allows us to obtain a signal with a higher signal-to-noise ratio.

Impact of relative position. Since different people have different storage habits, the relative positions of water cups and other items are different. To test the influence of different relative positions, we put the cup on the left front, left rear, right front, and right rear of the paper respectively for testing. Fig. 19 shows four relative positions. At each position, we collect 30 samples of each category shown in Fig. 13. We take the relative attenuation factor (using 4 frequencies) as features, and we can adopt a simple K-Nearest Neighbors algorithm ($K=1$) to differentiate those liquids. For each test, we use one situation of data as the test set and use other data to build the KNN classifier.

The identification results are shown in Fig. 18. It achieves accuracy over 94.03%. Compared with the change in the relative position of the antenna and the container, the change in the relative position of the container and other items has less influence on the accuracy of liquid identification. Because the different relative positions of the liquid to other objects are similar for both the signal reception and recognition models, this makes their accuracy less different.

6.2.4 Identify Liquids with Holding Freedom.

There are two basic requirements for holding freedom:

- (1) We can freely choose the container that holds the liquid. There are two typical container types that are placed in a packet: one is the beverage's packaging, and the other is our cup. We test both cases, and the cups we chose to consist of regular cylinders, irregular cylinders, and two types of cuboids with different bottom shapes, as shown in Fig. 11.

(2) The liquid detection is not affected by the height. On the one hand, we don't know how much liquid is originally in the container. Drinking, on the other hand, causes the liquid in the container to vary in height. In addition, tilting of the container can also cause the effective height of the liquid in the RF link to change. We test its ability to recognize liquids at different heights.

Impact of different types of cups. In addition, in order to test the influence of different shapes of cups on liquid identification, besides using the packaging of the beverage itself, we select 4 containers of different shapes for testing, including irregular cylinders (A), regular cylinders (B), a rectangular cuboid (C) with a square base and a rectangular cuboid (D) with a rectangular base, which are shown in Fig 11. For each case, we collect 30 samples of each category shown in Fig. 13. Having obtained the relative attenuation factor (using 4 frequencies) as features,

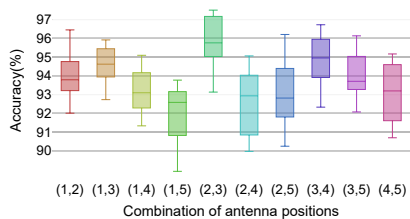


Fig. 22. The accuracy of placing the antenna in different positions.

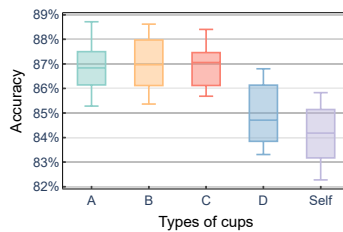


Fig. 23. The impact of different types of cups on recognition.

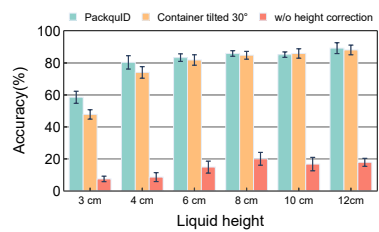


Fig. 24. The impact of different heights on liquid identification.



Fig. 25. Different experimental environments.

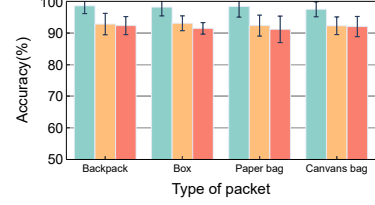


Fig. 26. Accuracy of liquid identification in different environments.

we can adopt a simple K-Nearest Neighbors algorithm ($K=1$) to differentiate those liquids. For each test, we use one cup of data as the test set and use other data to build the KNN classifier.

The identification results are shown in Fig. 23. It achieves an accuracy over 85.99%. This means it can identify liquids with high accuracy despite the material and shape of the containers. Furthermore, we notice that the three containers A, B, and C have similar accuracies, probably because they have similar shapes. In the process of the signal from the transmitting antenna to the receiving antenna, a beam of electromagnetic waves is actually transmitted in space instead of a ray. Different container shapes have different influence on the transmission of electromagnetic waves, which also results in the lowest average accuracy of identification when using the beverage's own packaging as the container for testing.

Impact of different heights of liquids. For testing the effect of the different liquid heights on identification, we use a cuboid resin container with a length of 10 cm for testing. We test 6 different heights including 3 cm, 4 cm, 6 cm, 8 cm, 10 cm and 12 cm. For each height, we collect data on 9 different common beverages, each beverage collect 50 times independently. We use a motor, which is shown in Fig. 21, to control the transmit antenna up or down. For each height, we collect data on when the container is upright and when the container is tilted 30 degrees. Having obtained the relative attenuation factor (using 4 frequencies) as features, we can adopt a simple K-Nearest Neighbors algorithm to differentiate those liquids. For each test, we use one height of data as the test set and use other data to build the KNN classifier. For example, if we test the accuracy of the system to identify the liquid when the liquid height is 4 cm, we use the data collected when the liquid height is 4 cm as the test data, and use the data collected when the liquid height is other values to construct the KNN classifier.

The results are shown in Fig. 24. We find that to ensure high accuracy, the liquid height needs to be greater than 4 cm. We believe the reason is the poor stability of the data when the motor is started. And when the liquid height is low, the duration of the signal containing the liquid information is short, which is not conducive to

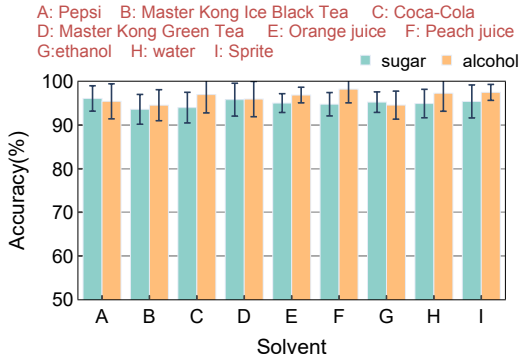


Fig. 27. Identify if the solvent contains other impurities.

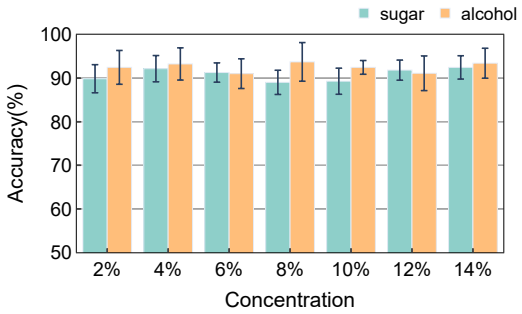


Fig. 28. Accuracy of concentration identification.

the screening of data for liquid identification. In addition, we test the results of directly extracting features for identification without high calibration, and we find that the accuracy is only 15.48%. This is because when the liquid height is lower than the antenna height, a part of the electromagnetic wave reaches the receiving antenna without passing through the liquid. The proportion of this part of the electromagnetic wave is affected by the height of the liquid, so the accuracy of identifying the liquid using the unprocessed signal is poor. And *PackquID* can extract the signal passing through the liquid transmission part, so it can identify the liquid independent of height. The inclination of the container affects the transmission distance of the signal in the liquid, and *PackquID* can identify liquid independent of the width of the container, so the tilting of the container does not make a big difference to the accuracy.

PackquID's performance in different environments with different packets. As shown in Fig. 25, we test the performance of *PackquID* in a hall environment, a corridor environment, and a laboratory environment. In each environment, we pour the 9 different liquids into 4 different packets, including backpack, canvas bag, paper bag, and box. For each liquid we collect data 30 times independently. As shown in Fig. 26, in different environments, the difference in the accuracy of liquid identification is less than 5%.

6.3 Case Study

In this section, we conduct two interesting case studies which are common in daily life: (1) We use *PackquID* to detect if there is extra sugar or alcohol added to the drink. (2) We utilize *PackquID* to identify fine-grained sugar or alcohol content in beverages.

Case 1: Whether there is extra sugar or alcohol in the drink? In many scenarios (such as controlling the alcohol intake of minors), we need to pay attention to whether there is additional alcohol or sugar in the beverage. People sometimes refer to alcohol and mixes in beverages (e.g. rum can be referenced mixed in Cola). Therefore, we first test *PackquID*'s ability to identify impurities (alcohol or sugar) in beverages. For nine common beverages, we collect data on when they are free of impurities and when they contain 10% sugar or alcohol. Data are collected 30 times independently for each condition. Then use the KNN ($k=1$) algorithm for liquid identification. The results are shown in Fig. 27, in 9 different solvents, the accuracy rate of impurity identification exceeds 95%. This suggests that *PackquID* can help us determine whether a drink has been added with extra alcohol or sugar.

Case 2: Fine-grained sugar or alcohol content in beverages. In order to eat scientifically, we usually need to control the intake of sugar and alcohol, which is especially important for patients with diabetes and the like. In addition, spoiled juices often contain alcohol due to fermentation, which means that fine-grained identification of alcohol concentration can help us determine whether the juice is spoiled. To test *PackquID*'s ability to perform concentration identification, we spike nine different beverages with sugar and alcohol at concentrations ranging

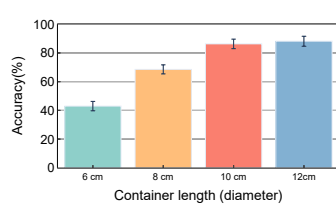


Fig. 29. Influence of container diameter on recognition accuracy.

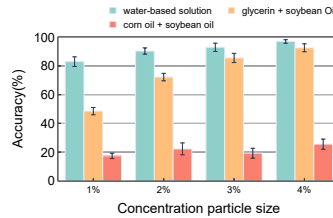


Fig. 30. The system has a stronger ability to identify solutions with polarity.

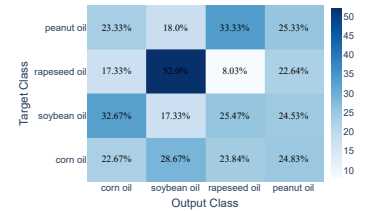


Fig. 31. The system is unable to differentiate between the 4 vegetable oils.

from 0 to 14% (2% intervals). Data are collected independently for 30 times in each case, and then identify the solute concentration in the liquid. The results are shown in Fig. 28. The recognition accuracy of concentration exceeds 90%. This means that *PackquID* has the opportunity to complete the fine-grained concentration-identification tasks by ubiquitous ways in life, helping us control sugar and alcohol intake.

6.4 Boundary of Liquid Identification Capability

We design experiments to test the boundaries of the *PackquID*'s ability to identify liquids. In order to effectively identify the liquid, the length of the container needs to be greater than 10 cm. Furthermore, since *PackquID* identifies liquids based on the attenuation of the signal in the liquid. Therefore, it has a stronger ability to identify liquids with strong polarity.

In order to effectively identify the liquid, the container radius needs to exceed 5 cm. To test the effect of container radius on the accuracy of liquid identification, we select 4 glass containers with different radius, including 4 cm, 6 cm, 8 cm and 12 cm. When testing, we set the height of the liquid to 12 cm. For each radius, we collect data on 9 different common beverages, each beverage collect 50 times independently. We perform data collection once a day for three days. Having obtained the relative attenuation factor (using 4 frequencies) as features, we can adopt a K-Nearest Neighbors algorithm to differentiate those liquids. We use five-fold cross-validation for testing. The results are shown in Fig. 29. We find that in order to ensure high recognition accuracy, the radius of the container should be greater than 10 cm. We believe that the reason is that when the radius of the container is large, the two receiving antennas (the radius of the antenna base is 1.5 cm) can be better shielded, so that the signal received mainly comes from the signal passing through the liquid. In future work, we plan to use smaller-sized antennas combined with beam-forming techniques to achieve liquid identification in smaller-sized containers. In addition, to ensure that the system can effectively identify liquids, the height of the liquid needs to be greater than 4 cm. Therefore, the minimum volume of liquid that the system can work with is approximately 320 ml.

For highly polar liquids, PackquID can be identified with a particle size of 2%. But it is difficult to identify for vegetable oils that are close to non-consumable media. We test the *PackquID*'s ability to identify different types of liquids. For water-based liquids with better conductivity, the system can achieve 2% particle size identification. Glycerol is dissolved in soybean oil that is approximately coal-free, and the particle size identified is 4%. For the dissolved corn oil in soybean oil, the system cannot effectively identify it.

We test the minimum particle size the system could recognize for different kinds of solutions. For water-based liquids, we use 9 common beverages (mineral water, Pepsi, Coca-Cola, and etc.) and sodium chloride (NaCl) as the solvent. For oil-based liquids, we use soybean oil as the solvent, and glycerol and corn oil as the solvent, respectively. For each solution, the solubility is varied from 0 to 20% with a concentration interval of 1%. Data are collected 50 times independently for each concentration. We test the system's ability to identify concentrations by selecting data at different concentration intervals. For example, when the granularity is 2%, we select two

sets of data: data with concentration 0, 2%, 4%,...,20%; and data with concentration 1%, 3%,...,19%. We then test the accuracy of the system in identifying concentrations using five-fold cross-validation. The results are shown in Fig. 30. For water-based liquids, the system can achieve 1% particle size identification. Our system can distinguish 2% particle size glycerol solutions with over 75% accuracy. But for the corn oil solution, the system has difficulty distinguishing effectively. We believe the reason is that the attenuation of electromagnetic waves is more pronounced in glycerol than in corn oil [3, 10, 13]. Since the liquid features we construct depend on the attenuation factor of the liquid, it is difficult to effectively distinguish between lossless media.

In addition, we test the system's ability to identify liquids that are nearly lossless media. We use 4 vegetable oils, including corn oil, soybean oil, canola oil, and peanut oil for testing. We partition the dataset using five-fold cross-validation and use the KNN classifier for liquid identification. The confusion matrix is shown in Fig. 31. We find that the system's ability to identify lossless media is weak.

7 RELATED WORK

7.1 Material Identification

7.1.1 Traditional Liquid Identification Methods. Traditionally, material identification requires the use of expensive specialized equipment to provide data [5, 18, 51, 53, 56]. The feasibility of these methods stems from a basic observation: different materials absorb and reflect light waves to different degrees. In addition to expensive equipment, these methods typically require the immersion of a probe in a liquid to collect the signal and use a spectrometer to further analyze the spectral information. This makes it unsuitable for ubiquitous applications in daily life, such as detecting liquids in packets.

7.1.2 RF-based Liquid Detection Method. Recently, *Reflected signal*, such as millimeter-wave radar and RFID, are used to detect liquids. Tagtag [63] sticks an RFID tag on the surface of the material to be tested (such as a milk box). Due to the existence of near-field coupling, when different kinds of liquids are placed in the container, the impedance of the RFID tag will change differently, which is used to construct the liquid signature. Similarly, RF-EATS [24] completes material identification by identifying the effect of different materials on the impedance of the backscatter tag and designs a migration network to make the system suitable for different application scenarios (e.g. identifying fake wine and identifying fake milk powder). FG-LiquID [37] designs a novel neural network for sensing liquids using millimeter-wave radar, which can identify 30 different liquids in a fine-grained manner. All of them have achieved good experimental results but are limited by the working mechanism of the reflected signal, these methods require that there should be no other objects between the signal receiver and the target to be measured. This limits their applications, such as backpacks that typically contain notebooks, books, or clothing in addition to liquids. In addition, many methods based on *transmitted signals* have been proposed. The key opportunity stems from the fact that due to the different complex permittivity of different liquids, the wave speed and degree of attenuation of the signal as it travels through the liquid are also different. Tagscan [58] places the liquid to be tested between the RFID antenna and the tags and uses the antenna to receive the reflected signal transmitted through the liquid. And it uses the RSSI and phase of the RFID signal to construct material features to complete the identification of 10 liquid materials. But it requires placing the liquid in a specific container. LiquID [15] uses the amplitude and phase of the signal to solve the equation to obtain the complex permittivity of the liquid, which is able to identify 33 kinds of liquids. Using mechanical waves, Vi-Liquid [26] builds a model to compute the viscosity of the liquid, which realizes the identification of 30 kinds of liquids. But these methods usually rely on prior knowledge, such as the material and width of the container. WiMi[19] utilizes the differential of the dual antennas to eliminate the effect of the container width. However, all of them are not suitable for liquid identification when both liquid and solid objects are present in the RF link.

They only identify liquids in the 2D ranges without considering the relative height of the liquid to the antenna. mSense [60] uses millimeter wave technology to achieve high-precision (90% accuracy) recognition of 5 materials

Table 1. Comparison of Liquid Identification Methods with Wireless Signals.

Method	Blocked by other items	Liquid location unknown	W/o prior knowledge	No specific container required	Liquid height unknown	Container
TagTag [63]	N/A ¹	no ²	yes	no	no	5500 ml
RF-EATS [24]	N/A	no	yes	no	no	N/A
FG-LiquID [37]	N/A	no	yes	no	no	400 ml
OSL [59]	N/A	no	yes	no	no	N/A
mSense [60]	N/A	no	yes	yes	yes	N/A
TagScan [58]	N/A	no	yes	no	no	9000 ml
WiMi[19]	no	no	no	yes	no	3700 ml
LiquID [15]	no	no	yes	no	no	2700 ml
Vi-Liquid [26]	no	no	yes	no	no	500 ml
<i>PackquID</i>	yes	yes	yes	yes	yes	320 ml

¹ N/A means the method is not applicable.

² no means not mentioned in the paper.

in mobile scenes, which means that it can achieve material recognition in the 3D range. However, limited by the principle of reflection perception, it cannot well adapt to the situation where there are other objects between the RF transceiver and the target to be measured. We constructed the distribution model of the electric field and eliminated the influence of height by using the change of the electric field when the transmitting antenna is displaced and completed the liquid recognition in the 3D range.

7.1.3 Optical and Camera-based Liquid Detection Method. Recent research on optical and camera-based liquid detection method has many different problem-solving theories and meaningful applications [25, 40, 45, 67]. Smart-U [25] can recognize food or liquid in the spoon by employing the LEDs and photodiodes. However, these methods are not easy to deploy in daily life. CapCam [67] uses the phone's camera to capture the ripples created by vibrations in the liquid to recognize them. But it only recognizes clear liquids.

7.2 Microwave Signal Based Sensing

With the development of 6G technology, the convergence of communication and perception is gaining increasing attention [12, 48]. Many of the signals in the microwave frequency band (e.g. WiFi and Bluetooth signals) that are common in our lives are used to perform sensing tasks. Compared with signals in the millimeter-wave band, microwave signals have stronger transmission capabilities and cheaper deployment costs in the medium. Hence, microwave signal based sensing has a huge amount of ubiquitous applications, including action identification [61, 69], localization and tracking [22, 64], user Identification [49], health monitoring [38, 68] and material identification [15, 19]. These researches verify the possibility of channel independent liquid identification.

7.3 Impedance Spectroscopy at RF

There are many ways to obtain the method related to the complex permittivity of liquids, including co-axial probe methods, free space methods, transmission line and reflection methods, resonant techniques [1]. A popular approach is using a co-axial probe dipped into the liquid while a vector network analyzer (VNA), connected to the probe, measures permittivity [42]. Although these methods can accurately obtain the complex permittivity of liquids, the equipment is expensive. Many lightweight liquid sensing tasks are not worth the exorbitant cost. Instead, *PackquID* provides a way to identify liquids using RF signals to construct features that are only related to the liquid's complex permittivity.

8 CONCLUSION AND FUTURE WORK

Conclusion. In this paper, we propose *PackquID*, which can accurately identify the liquid inside the packet with microwave signal. *PackquID* is a model-driven system and does not require prior knowledge of the channel (including the material and width of the container, the height of the liquid, the number and type of other items in the bag, etc.) to complete liquid identification. We test *PackquID*'s liquid identification performance in three different environments using 4 packets of different materials. For 4 different containers and 9 different beverages, the identification accuracy exceed 85%. Moreover, it can successfully distinguish extremely Beverages of similar alcohol content (with a 2% concentration difference). We believe *PackquID* could be a promising candidate for lightweight and universal liquid identification in daily life with numerous applications.

Future work. (1) We hope to combine WiFi technology and use mobile phones to achieve portable liquid detection. Currently we use a motor to control the transmitter antenna to move up and down to eliminate the effect of liquid height, which makes *PackquID* suitable for scenarios such as airport security checks that do not require frequent movement of devices. In the future, we hope to use handheld commercial devices such as smartphones to do this to improve the ease of use of in-packet liquid identification. At present, many smartphones have more than one WiFi antenna, and the latest standard of WiFi6 supports two frequency bands and supports more than 160 MHz bandwidth on each frequency band, which provide us the opportunity to port *PackquID* to commercial devices. (2) We hope to combine the phase information to complete the identification of the lossless medium. Since *PackquID* identifies liquids based on the attenuation of the signal, it is difficult to distinguish between non-consumable media (e.g vegetable oils). But previous research [15] has shown that different lossless media have different effects on the wave speed, which can lead to changes in the phase of the signal. We expect to combine phase features to enhance the system's ability to identify lossless media.

ACKNOWLEDGMENTS

The research is partially supported by China National Natural Science Foundation with No. 62132018, Key Research Program of Frontier Sciences, CAS. No. QYZDY-SSW-JSC002, The University Synergy Innovation Program of Anhui Province with No. GXXT-2019-024, and NSFC with No. 62072424, U20A20181.

REFERENCES

- [1] Mohammed Nurul Afsar, James R Birch, RN Clarke, and GW Chantry. 1986. The measurement of the properties of materials. *Proc. IEEE* 74, 1 (1986), 183–199.
- [2] Miklós Ajtai. 1994. The complexity of the pigeonhole principle. *Combinatorica* 14, 4 (1994), 417–433.
- [3] R Behrends, K Fuchs, U Kaatze, Y Hayashi, and Y Feldman. 2006. Dielectric properties of glycerol/water mixtures at temperatures between 10 and 50 C. *The Journal of chemical physics* 124, 14 (2006), 144512.
- [4] Mohammed Bendaoued, Jaouad Terhzaz, and Rachid Mandry. 2017. Determining the complex permittivity of building dielectric materials using a propagation constant measurement. *International Journal of Electrical and Computer Engineering* 7, 4 (2017), 1681.
- [5] CR Blakley, JJ Carmody, and ML Vestal. 1980. Liquid chromatograph-mass spectrometer for analysis of nonvolatile samples. *Analytical Chemistry* 52, 11 (1980), 1636–1641.
- [6] C Blom and J Mellema. 1984. Torsion pendula with electromagnetic drive and detection system for measuring the complex shear modulus of liquids in the frequency range 80–2500 Hz. *Rheologica acta* 23, 1 (1984), 98–105.
- [7] PP Bobrov, AS Lapina, and AV Repin. 2015. Effect of the rock/water/air interaction on the complex dielectric permittivity and electromagnetic waves attenuation in water-saturated sandstones. In *PIERS Proceedings*. 1877–1879.
- [8] Xavier Bohigas and Javier Tejada. 2010. Dielectric characterization of alcoholic beverages and solutions of ethanol in water under microwave radiation in the 1–20 GHz range. *Food research international* 43, 6 (2010), 1607–1613.
- [9] Roland Böhmer, M Maglione, Peter Lunkenheimer, and Alois Loidl. 1989. Radio-frequency dielectric measurements at temperatures from 10 to 450 K. *Journal of applied physics* 65, 3 (1989), 901–904.
- [10] MM Brady and SS Stuchly. 1981. Dielectric dispersion of glycerol from 2.0 to 4.0 GHz. *The Journal of Chemical Physics* 74, 6 (1981), 3632–3633.
- [11] Amir Ćenanović, Siegfried Martius, Andreas Kilian, Jan Schür, and Lorenz-Peter Schmidt. 2011. Non destructive complex permittivity determination of glass material with planar and convex surface. In *2011 German Microwave Conference*. IEEE, 1–4.

- [12] Shanzhi Chen, Ying-Chang Liang, Shaohui Sun, Shaoli Kang, Wench Cheng, and Mugen Peng. 2020. Vision, requirements, and technology trend of 6G: How to tackle the challenges of system coverage, capacity, user data-rate and movement speed. *IEEE Wireless Communications* 27, 2 (2020), 218–228.
- [13] Julián Corach, Eriel Fernández Galván, Patricio Aníbal Sorichetti, and Silvia Daniela Romano. 2019. Estimation of the composition of soybean biodiesel/soybean oil blends from permittivity measurements. *Fuel* 235 (2019), 1309–1315.
- [14] Juan de Vicente, Modesto T López-López, Juan DG Durán, and Fernando González-Caballero. 2004. Shear flow behavior of confined magnetorheological fluids at low magnetic field strengths. *Rheologica acta* 44, 1 (2004), 94–103.
- [15] Ashutosh Dhekne, Mahanth Gowda, Yixuan Zhao, Haitham Hassanieh, and Romit Roy Choudhury. 2018. Liquid: A wireless liquid identifier. In *Proceedings of the 16th Annual International Conference on Mobile Systems, Applications, and Services*. 442–454.
- [16] Paola Donato, Francesco Cacciola, Peter Quinto Tranchida, Paola Dugo, and Luigi Mondello. 2012. Mass spectrometry detection in comprehensive liquid chromatography: basic concepts, instrumental aspects, applications and trends. *Mass spectrometry reviews* 31, 5 (2012), 523–559.
- [17] Ugo Fano. 1947. Ionization yield of radiations. II. The fluctuations of the number of ions. *Physical Review* 72, 1 (1947), 26.
- [18] John F Federici. 2012. Review of moisture and liquid detection and mapping using terahertz imaging. *Journal of Infrared, Millimeter, and Terahertz Waves* 33, 2 (2012), 97–126.
- [19] Chao Feng, Jie Xiong, Liqiong Chang, Ju Wang, Xiaojiang Chen, Dingyi Fang, and Zhanyong Tang. 2019. WiMi: Target material identification with commodity Wi-Fi devices. In *2019 IEEE 39th International Conference on Distributed Computing Systems (ICDCS)*. IEEE, 700–710.
- [20] Richard P Feynman, Robert B Leighton, and Matthew Sands. 2011. *The Feynman lectures on physics, Vol. I: The new millennium edition: mainly mechanics, radiation, and heat*. Vol. 1. Basic books.
- [21] Daniel Fleisch. 2008. *A student's guide to Maxwell's equations*. Cambridge University Press.
- [22] Wei Gong and Jiangchuan Liu. 2018. SiFi: Pushing the limit of time-based WiFi localization using a single commodity access point. *Proceedings of the ACM on Interactive, Mobile, Wearable and Ubiquitous Technologies* 2, 1 (2018), 1–21.
- [23] David J Griffiths. 2005. Introduction to electrodynamics.
- [24] Unsoo Ha, Junshan Leng, Alaa Khaddaj, and Fadel Adib. 2020. Food and Liquid Sensing in Practical Environments using {RFIDs}. In *17th USENIX Symposium on Networked Systems Design and Implementation (NSDI 20)*. 1083–1100.
- [25] Qianyi Huang, Zhice Yang, and Qian Zhang. 2018. Smart-U: smart utensils know what you eat. In *IEEE INFOCOM 2018-IEEE Conference on Computer Communications*. IEEE, 1439–1447.
- [26] Yongzhi Huang, Kaixin Chen, Yandao Huang, Lu Wang, and Kaishun Wu. 2021. Vi-liquid: unknown liquid identification with your smartphone vibration.. In *MobiCom*. 174–187.
- [27] Akira Ishimaru. 2017. *Electromagnetic wave propagation, radiation, and scattering: from fundamentals to applications*. John Wiley & Sons.
- [28] Aravind Iyer, Catherine Rosenberg, and Aditya Karnik. 2009. What is the right model for wireless channel interference? *IEEE Transactions on Wireless Communications* 8, 5 (2009), 2662–2671.
- [29] John David Jackson. 1999. Classical electrodynamics.
- [30] Shan Jiang and Stavros Georgakopoulos. 2011. Electromagnetic wave propagation into fresh water. *Journal of Electromagnetic Analysis and Applications* 2011 (2011).
- [31] Udo Kaatze. 1989. Complex permittivity of water as a function of frequency and temperature. *Journal of Chemical and Engineering Data* 34, 4 (1989), 371–374.
- [32] John G Kirkwood. 1936. On the theory of dielectric polarization. *The Journal of Chemical Physics* 4, 9 (1936), 592–601.
- [33] John G Kirkwood. 1939. The dielectric polarization of polar liquids. *The Journal of Chemical Physics* 7, 10 (1939), 911–919.
- [34] John D Kraus and Ronald J Marhefka. 2011. Antenna: For all applications (Third Editions)[M]. Beijing, Publishing House Of Electronics Industry (2011).
- [35] Jerzy Krupka. 2006. Frequency domain complex permittivity measurements at microwave frequencies. *Measurement Science and Technology* 17, 6 (2006), R55.
- [36] Youbok Lee et al. 2003. Antenna circuit design for RFID applications. *AN710, Microchip Technology Inc* (2003).
- [37] Yumeng Liang, Anfu Zhou, Huanhuan Zhang, Xinzhe Wen, and Huadong Ma. 2021. FG-LiquID: A Contact-less Fine-grained Liquid Identifier by Pushing the Limits of Millimeter-wave Sensing. *Proceedings of the ACM on Interactive, Mobile, Wearable and Ubiquitous Technologies* 5, 3 (2021), 1–27.
- [38] Chen Liu, Jie Xiong, Lin Cai, Lin Feng, Xiaojiang Chen, and Dingyi Fang. 2019. Beyond respiration: Contactless sleep sound-activity recognition using RF signals. *Proceedings of the ACM on Interactive, Mobile, Wearable and Ubiquitous Technologies* 3, 3 (2019), 1–22.
- [39] Haitao Liu, Hao Tian, and Haifeng Cheng. 2013. Dielectric properties of SiC fiber-reinforced SiC matrix composites in the temperature range from 25 to 700° C at frequencies between 8.2 and 18 GHz. *Journal of nuclear materials* 432, 1-3 (2013), 57–60.
- [40] Hidenori Matsui, Takahiro Hashizume, and Koji Yatani. 2018. Al-light: An alcohol-sensing smart ice cube. *Proceedings of the ACM on Interactive, Mobile, Wearable and Ubiquitous Technologies* 2, 3 (2018), 1–20.

- [41] Igor S Nefedov, Ari J Viitanen, and Sergei A Tretyakov. 2005. Electromagnetic wave refraction at an interface of a double wire medium. *Physical Review B* 72, 24 (2005), 245113.
- [42] Agilent Application Note. 2006. Agilent basics of measuring the dielectric properties of materials. *Agilent literature number* (2006), 1–34.
- [43] Charles Herach Papas. 2014. *Theory of electromagnetic wave propagation*. Courier Corporation.
- [44] Dragan Poljak, Sinisa Antonijevic, Khalil El Khamlichi Drissi, and Kamal Kerroum. 2010. Transient response of straight thin wires located at different heights above a ground plane using antenna theory and transmission line approach. *IEEE transactions on electromagnetic compatibility* 52, 1 (2010), 108–116.
- [45] Tauhidur Rahman, Alexander T Adams, Perry Schein, Aadhar Jain, David Erickson, and Tanzeem Choudhury. 2016. Nutrilyzer: A mobile system for characterizing liquid food with photoacoustic effect. In *Proceedings of the 14th ACM Conference on Embedded Network Sensor Systems CD-ROM*. 123–136.
- [46] Christian Riesch, Erwin K Reichel, Franz Keplinger, and Bernhard Jakoby. 2008. Characterizing vibrating cantilevers for liquid viscosity and density sensing. *Journal of sensors* 2008 (2008).
- [47] Lior Rokach and Oded Maimon. 2005. Clustering methods. In *Data mining and knowledge discovery handbook*. Springer, 321–352.
- [48] Walid Saad, Mehdi Bennis, and Mingzhe Chen. 2019. A vision of 6G wireless systems: Applications, trends, technologies, and open research problems. *IEEE network* 34, 3 (2019), 134–142.
- [49] Muhammad Shahzad and Shaohu Zhang. 2018. Augmenting user identification with WiFi based gesture recognition. *Proceedings of the ACM on Interactive, Mobile, Wearable and Ubiquitous Technologies* 2, 3 (2018), 1–27.
- [50] Andrew Shaw, AI Al-Shamma'a, SR Wylie, and D Toal. 2006. Experimental investigations of electromagnetic wave propagation in seawater. In *2006 european microwave conference*. IEEE, 572–575.
- [51] Chenjun Shi, Ji Zhu, Mingqian Xu, Xu Wu, and Yan Peng. 2020. An Approach of Spectra Standardization and Qualitative Identification for Biomedical Materials Based on Terahertz Spectroscopy. *Scientific Programming* 2020 (2020).
- [52] F Stern and C Weaver. 1970. Dispersion of dielectric permittivity due to space-charge polarization. *Journal of Physics C: Solid State Physics* 3, 8 (1970), 1736.
- [53] Monika Szymańska-Chargot, Justyna Cybulska, and Artur Zdunek. 2011. Sensing the structural differences in cellulose from apple and bacterial cell wall materials by Raman and FT-IR spectroscopy. *Sensors* 11, 6 (2011), 5543–5560.
- [54] John Terry and Juha Heiskala. 2002. *OFDM wireless LANs: A theoretical and practical guide*. Sams publishing.
- [55] David Tse and Pramod Viswanath. 2005. *Fundamentals of wireless communication*. Cambridge university press.
- [56] Georgios Tsimimis, Fenghong Chu, Stephen C Warren-Smith, Nigel A Spooner, and Tanya M Monro. 2013. Identification and quantification of explosives in nanolitre solution volumes by Raman spectroscopy in suspended core optical fibers. *Sensors* 13, 10 (2013), 13163–13177.
- [57] Hippel AR Von and R Arthur. 1954. Dielectrics and waves.
- [58] Ju Wang, Jie Xiong, Xiaojiang Chen, Hongbo Jiang, Rajesh Krishna Balan, and Dingyi Fang. 2017. TagScan: Simultaneous target imaging and material identification with commodity RFID devices. In *Proceedings of the 23rd Annual International Conference on Mobile Computing and Networking*. 288–300.
- [59] Jonas Weiß and Avik Santra. 2018. One-shot learning for robust material classification using millimeter-wave radar system. *IEEE sensors letters* 2, 4 (2018), 1–4.
- [60] Chenshu Wu, Feng Zhang, Beibei Wang, and KJ Ray Liu. 2020. mSense: Towards mobile material sensing with a single millimeter-wave radio. *Proceedings of the ACM on Interactive, Mobile, Wearable and Ubiquitous Technologies* 4, 3 (2020), 1–20.
- [61] Dan Wu, Ruiyang Gao, Youwei Zeng, Jinyi Liu, Leye Wang, Tao Gu, and Daqing Zhang. 2020. FingerDraw: Sub-wavelength level finger motion tracking with WiFi signals. *Proceedings of the ACM on Interactive, Mobile, Wearable and Ubiquitous Technologies* 4, 1 (2020), 1–27.
- [62] Dan Wu, Daqing Zhang, Chenren Xu, Hao Wang, and Xiang Li. 2017. Device-free WiFi human sensing: From pattern-based to model-based approaches. *IEEE Communications Magazine* 55, 10 (2017), 91–97.
- [63] Binbin Xie, Jie Xiong, Xiaojiang Chen, Eugene Chai, Liyao Li, Zhanyong Tang, and Dingyi Fang. 2019. Tagtag: material sensing with commodity RFID. In *Proceedings of the 17th Conference on Embedded Networked Sensor Systems*. 338–350.
- [64] Huatao Xu, Dong Wang, Run Zhao, and Qian Zhang. 2019. AdaRF: Adaptive RFID-based indoor localization using deep learning enhanced holography. *Proceedings of the ACM on Interactive, Mobile, Wearable and Ubiquitous Technologies* 3, 3 (2019), 1–22.
- [65] Ruey-Bin Yang, Wen-Shyong Kuo, and Heng-Chih Lai. 2014. Effect of carbon nanotube dispersion on the complex permittivity and absorption of nanocomposites in 2–18 GHz ranges. *Journal of Applied Polymer Science* 131, 21 (2014).
- [66] Hui-Shyong Yeo, Gergely Flamich, Patrick Schrempp, David Harris-Birtill, and Aaron Quigley. 2016. Radarcat: Radar categorization for input & interaction. In *Proceedings of the 29th Annual Symposium on User Interface Software and Technology*. 833–841.
- [67] Shichao Yue and Dina Katabi. 2019. Liquid testing with your smartphone. In *Proceedings of the 17th Annual International Conference on Mobile Systems, Applications, and Services*. 275–286.
- [68] Youwei Zeng, Dan Wu, Jie Xiong, Jinyi Liu, Zhaopeng Liu, and Daqing Zhang. 2020. MultiSense: Enabling multi-person respiration sensing with commodity wifi. *Proceedings of the ACM on Interactive, Mobile, Wearable and Ubiquitous Technologies* 4, 3 (2020), 1–29.
- [69] Yue Zheng, Yi Zhang, Kun Qian, Guidong Zhang, Yunhao Liu, Chenshu Wu, and Zheng Yang. 2019. Zero-effort cross-domain gesture recognition with Wi-Fi. In *Proceedings of the 17th Annual International Conference on Mobile Systems, Applications, and Services*. 313–325.